Alternating-current losses in two-layer superconducting cables consisting of second-generation superconductors coated by U-shaped ferromagnetic materials*

Ahmet Cicek[a], Fedai Inanir[b]†, and Fedor Gömöry[c]

[a] Department of Physics, Faculty of Arts and Sciences, Mehmet Akif Ersoy University, Campus 15100, Burdur/Turkey
[b] Department of Physics, Faculty of Arts and Sciences, Recep Tayyip Erdoğan University, 53100, Rize/Turkey
[c] Institute of Electrical Engineering, Slovak Academy of Sciences, Dúbravská Cesta 9, 842 39 Bratislava, Slovakia

(Received 9 April 2013; revised manuscript received 8 May 2013)

Alternating-current losses in a two-layer superconducting cable, each layer being composed of 15 closely-spaced rectangular wires made up of second-generation superconductors when the ends of wires are coated by either a non-magnetic or strong ferromagnetic material having a U profile is numerically investigated. Computations are carried out through the finite-element method. The alternating-current losses do not increase significantly if the relative permeability of the coating is increased three orders of magnitude, provided that the current amplitude is less than half of the critical current in a superconducting wire. However, the losses are much higher for ferromagnetic coating if the amplitude of the applied current oscillating at 50 Hz is close to the critical current. The ferromagnetic coating is seen to accumulate the magnetic field lines normally on its surfaces, while the field lines are parallel to the long axes of the wires, leading to more significant flux penetration in the coated regions. This facilitates a uniform low-loss current flow in the uncoated regions of the wires. In contrast, coating with a non-magnetic material gives rise to a considerably smaller current flow in the uncoated regions, whereas the low-loss flow is maintained in the coated regions. Moreover, the current flows in opposite directions in the coated and uncoated regions, where the direction in each region is converse for the two materials.

Keywords: second-generation superconductor, two-layer cable, ferromagnetic coating, U profile, alternating-current losses

PACS: 84.71.Mn, 74.78.−w, 74.25.F− **DOI:** 10.1088/1674-1056/22/12/128403

1. Introduction

Superconducting cables are most widely used in power systems and fusion reactors.[1–5] Recently, high-temperature superconductors (HTS) are also extensively utilized in areas such as magnetic-resonance imaging (MRI), fault current limiters, and magnetic energy storage.[6–10] The determinant in all these applications is alternating-current (AC) losses, to reduce whom a number of methods have been developed or proposed. Two approaches at the forefront are modifying either the circumstances which influence the superconductor's physical parameters or the configuration of the superconductors forming the windings.[11–19]

The major loss in power transmission cables comes from the transport AC loss and influence their efficiency and economic feasibility. Therefore, it is crucial to understand and evaluate the AC loss behavior of HTS cables. Design and optimization of HTS cables are costly and time-consuming processes. The finite-element method (FEM) has been extensively utilized in predicting AC loss characteristics of cables and their optimization.[20–24] Although it is generally presumed that second-generation HTS tapes with magnetic substrate give rise to higher transport current loss compared to those with non-magnetic substrate, they can be preferred to reduce the manufacturing cost of cables in comparison to non-magnetic substrates (e.g., Hastelloy).

Numerous works have been carried out on the current distribution and AC losses in mono-layer HTS cables consisting of wires coated with a ferromagnetic material using FEM to determine the influences of the coating's magnetism on the superconducting layer.[25–29] Amemiya *et al.*[30] conducted numerical AC-loss calculations of two-layer HTS power transmission cables comprising of coated wires with a ferromagnetic material with respect to the arrangement of coated wires about the cable axis. Clem and Malozemoff[31] proposed a theory of AC transport loss in HTS power transmission cables comprising of second-generation wires coated with a magnetic substrate. Krüger *et al.*[32] studied magnetization losses in second-generation superconductors coated by ferromagnetic materials in the form of a horseshoe, where they reported that coating ends with ferromagnetic materials reduces losses. Similarly, Safran *et al.*[33] and Gömöry *et al.*[34] demonstrated both experimentally and numerically that coating with ferromagnetic materials remarkably reduces magnetization losses in first-generation Bismuth strontium calcium copper oxide (BSCCO) strips. Gömöry *et al.*[35] indicated that AC losses in the superconducting part of a tape coated by a horse-shoe-shaped ferromagnetic material decreases dramatically for magnetic field strentghs below the penetration field.

*Project supported by the Fund from the Scientific and Technological Research Council of Turkey (TÜBİTAK) (Grant No. 110T876).
†Corresponding author. E-mail: inanir@ktu.edu.tr
© 2013 Chinese Physical Society and IOP Publishing Ltd

Investigations of transport current losses in multi-layer cables when the wires are coated with ferromagnetic materials having a U profile on their ends have not been carried out. This work focuses on investigations of AC transport losses in two-layer superconducting cables in order to elucidate the influences of the ferromagnetic coating with a U profile.

2. Cable design and computational method

Figure 1 depicts the investigated circular two-layer HTS cable with an inner and outer radii of $R_{\rm i}$ and $R_{\rm o}$, respectively. A layer is composed of $N = 15$ second-generation HTS wires of rectangular cross-sectional area in the xy plane, each coated by a ferromagnetic material. The wires have an infinite extent along the z direction, where spiral winding of the wires is not taken into account. The innermost core, of radius $R_{\rm i}$, is made up of copper (Cu). The space between the cable layers is filled with Kapton® dielectric, whereas the outer region, $r > R_{\rm o}$, is vacuum. Descriptions and values of the geometrical parameters of the cable can be found in Table 1, which also lists the physical parameters adopted in the computations.

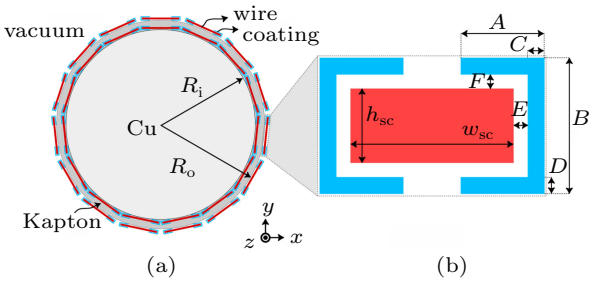


Fig. 1. (color online) Design of the two-layer HTS cable (a) and definitions of the geometrical parameters on each constituent wire coated by ferromagnetic material (b). The wires are not drawn to scale for clarity.

Each wire in Fig. 1 is coated by U-shaped ferromagnetic materials on its ends along the azimuthal direction, so that a spacing of $h_{\rm B} = 0.1$ μm between the wire and coating layer, corresponding to an oxide layer, exists. The thickness of the coating layer is $h_{\rm T} = 80.0$ μm. The other coating parameters, as a function of $h_{\rm B}$ and $h_{\rm T}$ are listed in Table 1. The relative permeability ($\mu_{\rm r}$) of the coating is taken as either 1.0 or 5.0×10^3, corresponding to non-magnetic and strong ferromagnetic substances, respectively.

Table 1. List of geometrical and physical parameters employed in computations.

Quantity (unit)	Description	Value
$I_{\rm c}$/A	critical current	2400
A_n	scaling parameter	1.80×10^{-7}
$w_{\rm sc}$/mm	width of an HTS wire	4.00
$h_{\rm sc}$/μm	height of an HTS wire	2.00
A/mm	extent of coating over a wire	1.08 ($= w_{\rm sc}/4 + h_{\rm B} + h_{\rm T}$)
B/μm	height of ferromagnetic coating	162.20 ($= 2(h_{\rm B} + h_{\rm T}) + h_{\rm sc}$)
C, D/μm	thickness of ferromagnetic coating	80.00 ($= h_{\rm T}$)
E, F/μm	spacing between coating and a wire	0.10 ($= h_{\rm B}$)
$R_{\rm i}$/mm	inner cable radius	19.98
$R_{\rm o}$/mm	outer cable radius	20.93
$R_{\rm CD}$/mm	radius of computational domain	25.00

Investigations are based on two-dimensional FEM simulations implemented through the AC/DC module of the Comsol MultiPhysics package.[36] Due to the periodicity of the system, the computational domain is a circular arc of $2\pi/N$ angular extent with a radius of $R_{\rm CD}$. The superconducting regions in the computational domain are meshed with quadrilateral elements of a 20/2100 height/width ratio, while the ferromagnetic material, the dielectric, and the free-space regions are meshed with triangular elements. The total number of nodes in each simulation is 102715, whereas the number of elements is 145361 (85361 triangular and 60000 quadrilateral). This choice results in a minimum mesh quality of 0.572. The meshing scheme is maintained between computational runs in order for ease of comparison between the obtained results.

In computations, a sinusoidally-varying current with a frequency of $f = 50$ Hz having constant amplitude is applied to all wires. Dependence of the critical current on magnetic field is ignored. Current is applied along the z direction, while the cable rests in the xy plane. Thus, the independent variables in the problem are J_z and A_z, the current density and the vector potential along the z direction, respectively. The boundary condition in FEM simulations is adopted as the vector potential produced by a superconducting strip, on which a current of $I_{\rm a}$ flows along the z direction, at a distance of $r = (x^2 + y^2)^{1/2}$:[35]

$$A_r = -\frac{\mu_0 I_{\rm a}}{2\pi}\left(\ln\left(\frac{r}{R_{\rm i} + h_{\rm SC}}\right) + \ln\left(\frac{r}{R_{\rm o} + h_{\rm SC}}\right) + 2\right). \quad (1)$$

Further details of the calculations can be found elsewhere.[15,35,37] The AC losses in the cable in Fig. 1 can be calculated by applying a current to the superconductor over a whole period (T). The applied current frequency is generally on the order of 1 Hz. However, the application of a 50 Hz-current does not considerably influence the AC-loss curves. Thus, the sampling frequency, f, is taken as 50 Hz and the current is applied in a duration between $T/4$ and $3T/4$ of the current, where 8 different current amplitudes ranging between 7% and 90% of the critical current, $I_{\rm c}$, are considered. The

transient analyses employ the solution obtained in the previous, t_{i-1}, time step to calculate the solution at time t_i. In this case, the derivative of the vector potential, A_z, with respect to time can be approximated as

$$\frac{\partial A_z(x,y)}{\partial t} \cong \left(\frac{A_z(x,y,t_i) - A_z(x,y,t_{i-1})}{\Delta t}\right), \tag{2}$$

where $\Delta t = t_i - t_{i-1}$. The first $T/4$ period of the current cycle cannot be represented by the cycle regime. Thus, the computations are initialized at $T/4$ and cover the duration up to $3T/4$.

3. Results and discussion

The variation of AC transport loss in each superconducting wire with respect to the current amplitude, I_a, is presented in Fig. 2. The relation between the magnetic flux density inside the coating material and the magnetic field strength is taken as $B = \mu_0\mu_r H$, where the temperature and position dependence of the relative dielectric permeability, μ_r, is neglected. In this way, it is possible to investigate the AC losses only on the superconducting wires.

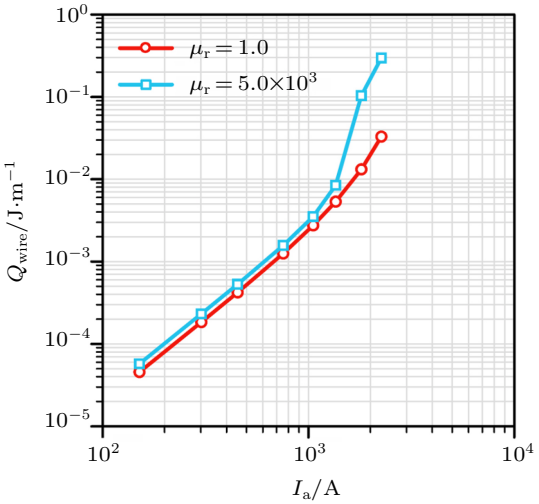


Fig. 2. (color online) Comparison of AC transport losses in a superconducting wire for different μ_r, as a function of the applied current amplitude.

Figure 2 compares $\mu_r = 1.0$ and $\mu_r = 5.0\times10^3$ cases. The AC loss can be obtained by using the calculated current values at each time step of the alternating-current cycle, the electric-field distribution or the vector potential. The most-widely utilized approach is calculating the AC current loss, $Q_{\rm wire}$, via the product of the current density and the electric field strength as $p = J \cdot E$, which is integrated over the cross-sectional area of the wire at a single time step, followed by an integral over the whole considered alternating-current cycle. Another method is calculating the total potential drop over the cable by averaging the gradient of the scalar electrical potential (the electric field), ΔV.[37]

The latter approach is implemented as follows: first, the applied current is sequentially decreased from I_a to $-I_a$ and then ΔV is calculated over the cross-sectional area of each wire. The gradient is constant throughout the wire cross section in the xy plane. Thus, its value at any point on the cross section can be taken into account. The gradient is, in turn, used to calculate the magnetic flux, Φ, across the wire. The dependency of Φ on the instantaneous value of the transport current over a cycle forms a hysteresis. The AC loss in each cycle in the wire is equal to the area of the hysteresis curve:[37]

$$Q_{\rm wire} = \oint \Phi {\rm d}I. \tag{3}$$

The existence of a strong ferromagnetic coating (with $\mu_r = 5.0\times10^3$) does not significantly increase the AC loss on a superconducting wire, Fig. 2. The AC loss increases linearly in the log–log scale of Fig. 2 for both the non-magnetic and strong ferromagnetic coatings, as I_a is increased up to approximately 55% of I_c. Actually, the discrepancy between the two cases is less than 1% in this current range. In contrast, the AC loss increase is much steeper for higher I_a, where the corresponding values are 0.03 J/m and 0.30 J/m for $\mu_r = 1.0$ and $\mu_r = 5.0\times10^3$, respectively, at approximately $0.9I_c$. The loss for the strong ferromagnetic material is an order of magnitude larger than the loss for the non-magnetic material at this current amplitude. Moreover, the ratio of the AC loss at $I_a = 0.9I_c$ for the strong ferromagnetic material is, again, an order of magnitude larger than the corresponding loss at $I_a = 0.1I_c$. The above facts suggest that the superconducting cable in Fig. 1 can be operated efficiently with low loss in a current regime where the amplitude is less than $I_c/2$.

The equi-potential contours of the magnetic vector potential, A_z, in the vicinity of the superconducting cable at $I_a = 0.9I_c$ is presented in Fig. 3. The densely-spaced contours around the ferromagnetic coating is mainly normal to the surface, while they are parellel to the superconducting wires away from the coatings, Fig. 3(b). This means that the ferromagnetic coating accumulates the contours on itself, whereas the contours are sparsely-spaced in the case of non-magnetic coating in Fig. 3(a). On the contrary, the field contours are non-normal to the surfaces of the non-magnetic coating in Fig. 3(a). Hence, the ferromagnetic coating facilitates alignment of the magnetic field lines parallel to the superconductor between the two cable layers. Thus, it can be expected that the AC losses are generally smaller in the uncoated regions.

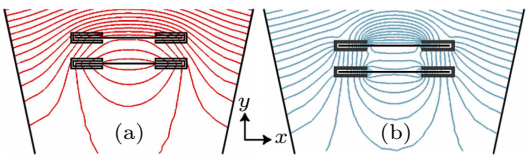


Fig. 3. (color online) Distribution of the magnetic vector potential field lines in the vicinity of the superconducting wires forming the two cable layers for non-magnetic (a) and strong ferromagnetic (b) coatings.

Distribution of the current density, J_z, on the cross sections of the superconducting wires is depicted in Fig. 4 for

an applied current of $I_a = 0.9I_c$. The current flows primarily across the coating region for the non-magnetic material, Fig. 4(a). In contrast, current mainly flows across the uncoated regions of the superconducting wires in the case of ferromagnetic coating, Fig. 4(b). Besides, current flows in the $+(-)z$ in the coated edges of the superconductors for the non-magnetic (ferromagnetic) coatings. Moreover, the current density distributions in Fig. 4 have minor discrepancies between the inner and outer superconducting wires.

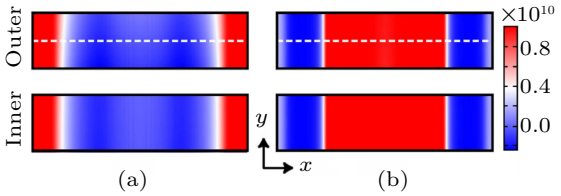


Fig. 4. (color online) Distribution of current density, J_z, (in A/m^2) over the cross section on the xy-plane of superconducting wires forming the two cable layers for non-magnetic (a) and strong ferromagnetic (b) coatings. The dashed horizontal lines represent the cuts along the x direction, over which the current distribution is investigated.

The current distributions in Fig. 4 are closely related to the magnetic-field line distributions in Fig. 3. Comparison of Fig. 3(b) and Fig. 4(b) reveals that current flow is obstructed in the regions where the magnetic field lines are normal to the superconductors' surfaces, so that more magnetic flux penetrates into the wires, in the case of ferromagnetic coating. Thus, the current varies significantly over the ferromagnetic-coated edges of the wires, whereas the current distribution is barely affected in the interiors, Fig. 4(b). The two cases can be contrasted by considering the ratio of the areas within the wires where the current density is close to its maximum, i.e. $A_R \equiv \text{Area}(\mu_r = 5.0\times10^3)/\text{Area}(\mu_r = 1.0)$. The A_R ratio is found out to be 2.51 for the investigated cable. Therefore, coating the superconducting wires on their ends by U-shaped ferrromagnetic materials may be a good candidate for both enhancing the mechanical strength and reducing the AC losses.

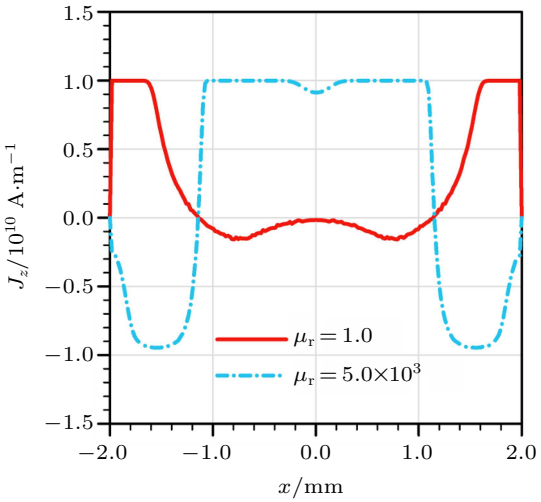


Fig. 5. (color online) Variation of current density on the denoted paths in Fig. 4 for the two coating materials.

Distribution of current density in one-dimension on the dashed cuts in Fig. 4 is presented in Fig. 5. In line with the above discussion, current distribution is more homogeneous in the central region of the ferromagnetic-coated wires. The current flowing in the reverse $(-z)$ direction beneath the ferromagnetic coating has a magnitude close to that of the applied current. In contrast, much smaller current in magnitude flows in the central region for the non-magnetic coating. In this case, the current distribution is homogeneous beneath the coatings.

4. Conclusion

Coating ends of the constituent superconducting wires of a two-layer circular cable with a ferromagnetic material is shown to have little influence on the alternating-current losses along the wires relative to the corresponding losses for coating with a non-magnetic material, provided that the applied current amplitude is less than half the critical current. The losses are much stronger in the case of ferromagnetic current for higher current amplitudes. The magnetic field lines penetrate more into the wires in the ferromagnetic coated regions, while the field lines are almost parallel to the wires in the region between the two layers. Accordingly, ferromagnetic coating facilitates more uniform and low-loss current flow in the uncoated regions of the wires.

References

[1] Ballarino A, Bauer P, Bi Y F, Devred A, Ding K Z, Foussat A, Mitchell N, Shen G, Song Y T, Taylor T, Yang Y F and Zhou T Z 2012 *IEEE Trans. Appl. Supercond.* **22** 4800304
[2] Barbero Soto E, Bellesia B, Bonito Oliva A, Boter E, Buskop J, Caballero J, Cornelis M, Cornella J, Galvan S, Losasso M, Poncet L, Harrison R, Heikkinen S, Rajainmaki H, Testoni P and Verpont A 2012 *IEEE Trans. Appl. Supercond.* **22** 4200206
[3] Furuse M, Okano M, Fuchino S, Uchida A, Fujihira J, Fujihira S, Kadono T, Fujimori A and Koide T 2012 *IEEE Trans. Appl. Supercond.* **22** 3900504
[4] Parkinson B J, Slade R, Mallett M J D and Chamritski V 2013 *IEEE Trans. Appl. Supercond.* **23** 4400405
[5] Zhang C W, Zhou L, Sulpice A, Soubeyroux J L, Verwaerde C, Gia Ky H, Zhang P X, Lu Y F and Tang X D 2007 *Chin. Phys.* **16** 1764
[6] Wang Q, Dai Y, Zhao B, Song S, Wang C, Li L, Cheng J, Chen S, Wang H, Ni Z, Li Y, Cui C, Hu X, Wang H, Lei Y, Chan K, Yan L, Wen C, Hui G, Yang W, Liu F, Zhuo Y, Zhou X, Yan Z, Chen J and Xu T 2012 *IEEE Trans. Appl. Supercond.* **22** 4400905
[7] Feng Z, Li L, Gao C, Zhu G, Li Y, Li X, Dai Y and Wang Q 2012 *IEEE Trans. Appl. Supercond.* **22** 4402206
[8] Zuijderduin R, Chevtchenko O, Smit J J Aanhaanen G, Melnik I and Geschiere A 2012 *Phys. Proc.* **36** 890
[9] Hobl A, Goldacker W, Dutoit B, Martini L, Petermann A and Tixador P 2013 *IEEE Trans. Appl. Supercond.* **23** 5601804
[10] Han Y H, Park B J, Jung S Y and Han S C 2012 *Physica C* **483** 156
[11] Grinenko V, Fuchs G, Nenkov K and Holzapfel B 2013 *Supercond. Sci. Technol.* **26** 035002
[12] Zhang P X, Inada R, Uno K, Oota A and Zhou L 2000 *Supercond. Sci. Technol.* **13** 1505
[13] Amemiya N, Li Q, Takeuchi K, Nakamura T, Yagi M, Mukoyama S, Aoki Y and Fujiwara N 2011 *IEEE Trans. Appl. Supercond.* **21** 943
[14] Amemiya N, Li Q, Ito K, Takeuchi K, Nakamura T and Okuma T 2011 *Supercond. Sci. Technol.* **24** 065013
[15] Gömöry F and İnanır F 2012 *IEEE Trans. Appl. Supercond.* **22** 4704704
[16] Malozemoff A P, Snitchler G and Mawatari Y 2009 *IEEE Trans. Appl. Supercond.* **19** 3115

[17] Stenvall A, Grilli F and Vojenčiak M 2011 *Supercond. Sci. Technol.* **24** 085016
[18] Siahrang M, Sirois F, Nguyen D N and Ashworth S P 2012 *Supercond. Sci. Technol.* **25** 014001
[19] Zhang G M, Lin L Z, Xiao L Y, Qiu M, Yu Y J and Hui D 2003 *Chin. Phys.* **12** 553
[20] Hong Z, Campbell A M and Coombs T A 2006 *Supercond. Sci. Technol.* **19** 1246
[21] Brambilla R, Grilli F, Martini L and Sirois F 2008 *Supercond. Sci. Technol.* **21** 105008
[22] Grilli F, Stavrev S, Le Floch Y, Costa Bouzo M, Vinot E, Klutsch I, Meunier G, Tixador P and Dutoit B 2005 *IEEE Trans. Appl. Supercond.* **15** 17
[23] Grilli F, Stavrev S, Dutoit B, Spreafico S, Tebano R, Gömöry F, Frolek L and Šouc J 2004 *Physica C* **401** 176
[24] Klincok B and Gömöry F 2006 *J. Phys.: Conf. Ser.* **43** 897
[25] Miyagi D, Wakatsuki T, Takahashi N, Torii S and Ueda K 2004 *IEEE Trans. Magn.* **40** 908
[26] Tsukamoto O, Liu M, Odaka S, Miyagi D and Ohmatsu K 2007 *Physica C* **463** 766
[27] Tsukamoto O, Sekizawa S, Alamgir A K M and Miyagi D 2007 *Physica C* **463** 770
[28] Miyagi D, Amadutsumi Y, Takahashi N and Tsukamoto O 2007 *Physica C* **463** 781
[29] Miyagi D, Umabuchi M, Takahashi N and Tsukamoto O 2007 *Physica C* **463** 785
[30] Amemiya N, Nakahata M, Fujiwara N and Shiohara Y 2010 *Supercond. Sci. Technol.* **23** 014022
[31] Clem J R and Malozemoff A P 2010 *Supercond. Sci. Technol.* **23** 034014
[32] Krüger P A C, Grilli F and Farinon S 2011 *Physica C* **471** 1083
[33] Safran S, Vojenčiak M, Gencer A and Gömöry F 2010 *IEEE Trans. Appl. Supercond.* **20** 2294
[34] Gömöry F, Šouc J, Vojenčiak M, Alamgir A K M, Han Z and Gu C H 2007 *Appl. Phys. Lett.* **90** 092506
[35] Gömöry F, Vojenčiak M, Pardo E, Solovyov M and Šouc J 2010 *Supercond. Sci. Technol.* **23** 034012
[36] Comsol Multiphysics v.4.2 (http://www.comsol.com)
[37] Gömöry F, Vojenčiak M, Pardo E and Šouc J 2009 *Supercond. Sci. Technol.* **22** 034017